J. Synchrotron Rad. (1999). **6**, 1–5

Diamond-based semi-transparent beam-position monitor for synchrotron radiation applications

P. Bergonzo,[a]* A. Brambilla,[a] D. Tromson,[a] R. D. Marshall,[a] C. Jany,[a] F. Foulon,[a] C. Gauthier,[b] V. A. Solé,[b] A. Rogalev[b] and J. Goulon[b]

[a]LETI (CEA-Technologies Avancées) DEIN/SPE, CEA/Saclay, 91191 Gif-sur-Yvette CEDEX, France, and [b]European Synchrotron Radiation Facility (ESRF), BP 20, F-38043 Grenoble CEDEX, France. E-mail: bergonzo@serin.cea.fr

(*Received 20 August 1998; accepted 17 November 1998*)

A soft X-ray beam-position monitor based on a thin CVD diamond photodetector has been developed for use on third-generation synchrotron radiation facilities, and has been tested on beamlines ID26 and ID12 at the European Synchrotron Radiation Facility. Since diamond exhibits a low absorption to low-energy X-ray photons, this device allows beam-position monitoring with very little beam attenuation at photon energies as low as 2 keV. The devices presented here find their use essentially on low-energy monochromatic beamlines with narrow beam sizes (typically below 1 mm^2). Measurements performed on a 20 μm-thick device show that a position sensitivity of 2 μm can readily be achieved with a photon flux attenuation of 22% at 4 keV. This allows permanent *in-situ* monitoring of beam instabilities during experiments.

Keywords: beam-position monitors; CVD diamond; X-rays; detectors.

1. Introduction

With the advances in experiments using third-generation synchrotron radiation sources, accurate control of the beam has become necessary. Conventional beam-position monitors (BPMs) based on semiconductor photodetectors typically exhibit a resolution of a few micrometres, but their inherent drawback is the complete absorption of the incoming radiation (Gauthier *et al.*, 1995). Their use is therefore restricted to apparatus calibration, as well as to beam-size or position-probing experiments. For demanding experiments, such as XAFS on ultradilute samples or polarization-dependent X-ray spectroscopy, it is necessary to control the beam instabilities with respect to both position and time. In order to measure the beam without significant attenuation, a low-absorption-cross-section detector is required. Therefore, with the low X-ray energies involved, a low-atomic-number semiconductor, such as diamond, will be required. We report here on the fabrication and use of such a device, to enable permanent monitoring and eventually compensation of beam-position shifts. Diamond interests for synchrotron-radiation monitoring have been demonstrated recently, where a perforated position-sensitive device exploiting the extreme thermal properties of diamond was developed (Sakae *et al.*, 1997).

2. Diamond-based BPMs

2.1. *Diamond material synthesis*

Diamond exhibits superior properties to other semiconducting materials, such as a high thermal conductivity, a high radiation hardness and a low thermal expansion coefficient, that enable its use as a radiation and photon detector (Franklin *et al.*, 1992; Kania *et al.*, 1990, 1993; Manfredotti *et al.*, 1994; Marinelli *et al.*, 1998). For the last few years we have investigated the growth of diamond towards the fabrication of radiation detection devices. We have recently reported its use for α and thermal neutron detection (Bergonzo *et al.*, 1998; Foulon, Bergonzo, Brambilla *et al.*, 1998), as well as for VUV laser photons (Foulon, Bergonzo, Borel *et al.*, 1998). Of the techniques available for synthesizing thin layers of diamond, it has recently been made feasible to produce material with good detection properties by chemical vapour deposition (CVD). From the dissociation of a gaseous precursor mixture consisting of methane diluted in hydrogen, it is possible to grow at high temperatures ($\sim$1073 K) a polycrystalline material on carbide forming materials such as silicon and over large areas. Of the commonly used energy sources applied to the gaseous mixture, microwave excitation is known to result in the production of materials with the best electronic properties and here a 2.45 GHz source was used to enable the growth of diamond on 5 cm silicon substrates. The material obtained has a polycrystalline structure with a grain size of the order of 10% of the layer thickness, and Raman analysis showed one intense peak at 1332 cm^{-1} and no other non-diamond carbon species. We have grown diamond using optimized growth conditions in order to obtain material with good electronic properties, that enable its use for detection applications (Jany, Bergonzo *et al.*, 1998). Typical growth rates are of the order of 0.5 μm h^{-1} for good quality films exhibiting the best

electronic properties and detection performances. After growth, a series of annealing steps and chemical treatments are performed in order to significantly improve the properties of the films (Jany, Foulon *et al.*, 1998). From the film deposited on the silicon substrate, it is possible to back etch a hole in the silicon in acid in order to obtain a thin diamond membrane supported by a silicon ring. Thin layers of diamond can be formed for detection purposes using this technique. At a typical thickness of 20 μm, a 1 cm-diameter membrane presents a good mechanical resilience that enables normal handling and transportation. Membranes as thin as 2 μm can be fabricated, but care has to be taken when handling them for vacuum applications since they can easily be shattered by the pressure differences encountered during rough pumping stages.

2.2. *X-ray cross sections*

Fig. 1 shows the calculated transmission coefficient of diamond layers of various thicknesses as a function of the incident energy in the 0.8 to 30 keV range. It can be observed that a 20 μm-thick film absorbs no more than 22% in the 4–10 keV range, thus making such a thickness ideal at this energy range. Above 10 keV, the absorption of a 20 μm-thick film remains below 2%, which may imply the need for thicker materials at low photon fluxes. Below 4 keV, a region where most materials are opaque, diamond is unique in that a 5 μm-thick film can permit 40% transmission at 1.5 keV.

2.3. *Principle of operation*

The principle of operation of the diamond BPM is shown in Fig. 2. Electrodes are positioned on both sides of the membrane and an external voltage is applied to produce an electric field in the device. When the photon flux interacts in the diamond, it generates free carriers (electrons and holes) that will drift along the electric field and induce a current in the external circuit. The BPMs fabricated here consist of a 20 μm-thick undoped polycrystalline diamond layer, prepared using the microwave-enhanced CVD technique using a process optimized for detection properties. The film was deposited on a silicon substrate which subsequently had the central area (8 mm diameter) chemically etched. Four 4 mm^2 gold pads of thickness 500 Å were evaporated on the top side to form electrodes, using the standard photolithographic techniques. The gap separating the electrodes is 0.5 mm. During normal operation, *i.e.* when the beam interacts between the four pads, the gold pads are not in the beam path. The back electrode covers the entire surface of the membrane and is made of a 500 Å-thick graphite layer. The contact material thicknesses used are too thin to induce any significant attenuation. When the X-ray beam directly illuminates a gold pad, no current can be measured unless the device is biased, implying ohmic contact behaviour on polycrystalline diamond (Gildenblat *et al.*, 1991). The detector was operated under a 100 V DC bias.

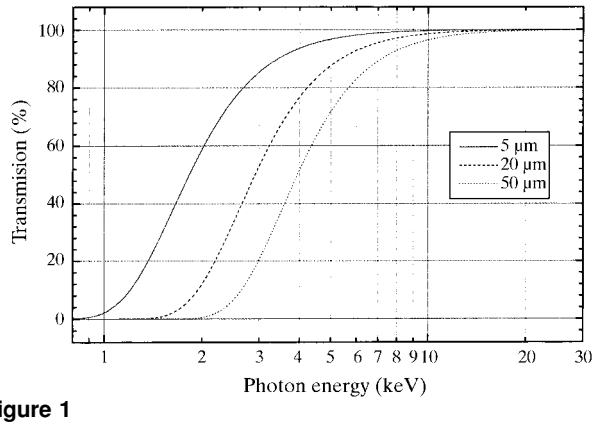

Figure 1
Transmission of diamond in the 0.8–30 keV range. Values are given for 5, 20 and 50 μm-thick diamond layers.

3. Experimental set-up and arrangements

3.1. *Beamline*

The experiments were performed at the ESRF on beamlines ID26 and ID12A, dedicated to XAFS on ultra-dilute samples and polarization-dependent X-ray spectroscopy, respectively. The electron ring was filed in the 16-bunch mode with an injection current of 65 mA. On each beamline the beam was monochromated using a double-crystal [Si(111)] fixed-exit Khozu monochromator. Harmonic rejection was performed using two silicon mirrors at grazing incidence. The experiments were performed at a fixed energy of 4 keV. The beam size was determined using high-accuracy copper slits that limit the beam to a region of high-intensity uniformity (<10%).

3.2. *Position measurement*

The four-quadrant position sensor was connected to an existing beam-position-monitoring four-channel electrometer (Gauthier *et al.*, 1995), and the DC bias was applied *via* the back graphite electrode. No additional modification from the routinely used beamline electronic set-ups was necessary for using the diamond BPM. The experiment was mounted on a table equipped with two translation stages. The BPM was able to move in the vertical and horizontal plane perpendicular to the beam.

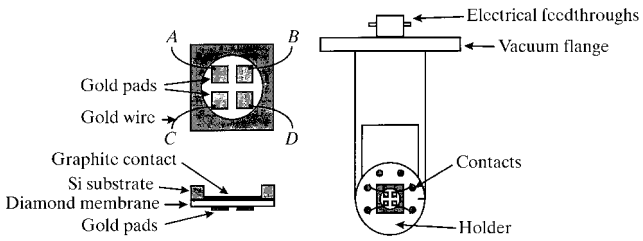

Figure 2
Schematic view of the diamond BPM (left), and complete device (right). The device can be mounted on a standard vacuum manipulator.

The X-ray spotlight was chopped at a frequency of 67 Hz and a lock-in amplifier was used in order to improve the signal-to-noise ratio and long-term stability, thus allowing the monitoring of lower beam intensities. The measurements were all obtained using an acquisition time of 1 s point^{-1}. The signals measured on each channel are normalized by dividing by the sum of the four-channel response currents. With this configuration the detector response is not influenced by variations of the beam intensity. From the current measured in each electrode, the beam gravity centre can be determined by using the standard relations

$$y = \frac{I(A) + I(D) - I(B) - I(C)}{I(A) + I(D) + I(B) + I(C)},$$

$$z = \frac{I(A) + I(B) - I(C) - I(D)}{I(A) + I(B) + I(C) + I(D)},$$

where y is the horizontal beam gravity centre position, z is the vertical beam gravity centre position and $I(n)$ is the net current in the electrode n ($n = A, B, C, D$; see Fig. 2).

4. Results

4.1. *Mapping of the BPM active area*

Fig. 3 shows a three-dimension representation of the detector response observed when a 200 µm × 200 µm square X-ray beam is scanned across the BPM. It represents the total current measured from the four electrodes as a function of the position of the beam centre. The monochromatic energy used for this measurement was 4 keV. No difference is observed when the beam enters the detector from the graphite side or from the gold side. The BPM

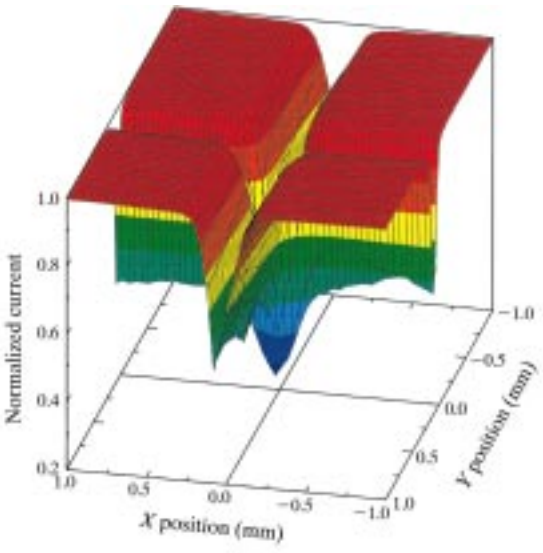

Figure 3
Three-dimensional representation of the detector response observed when a 200 µm × 200 µm square 4 keV X-ray beam is scanned across the BPM. In practice, the entire experimental set-up is moved around the beam using a hexapod table.

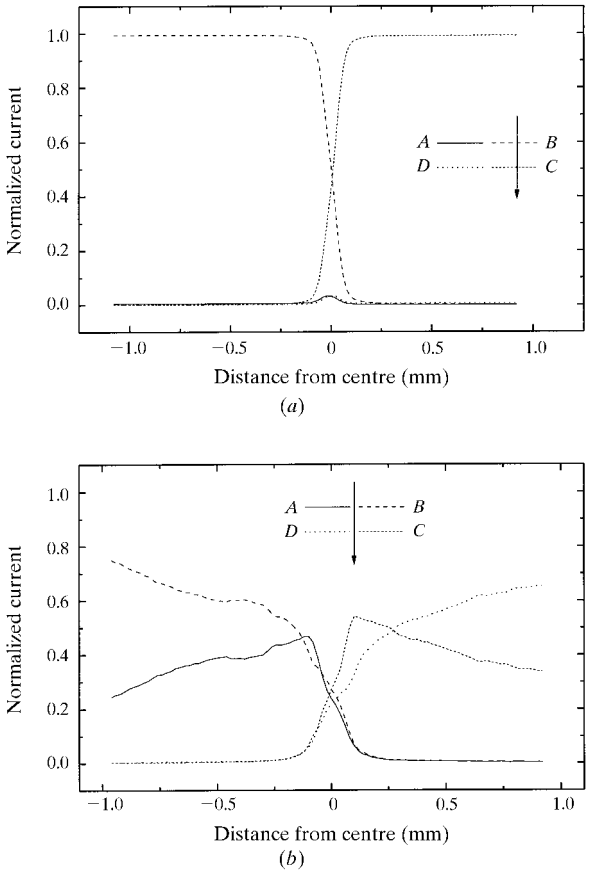

Figure 4
Plot of the normalized currents measured on the four electrodes as a function of the beam position. Beam energy is 4 keV, beam size is 200 µm × 200 µm.

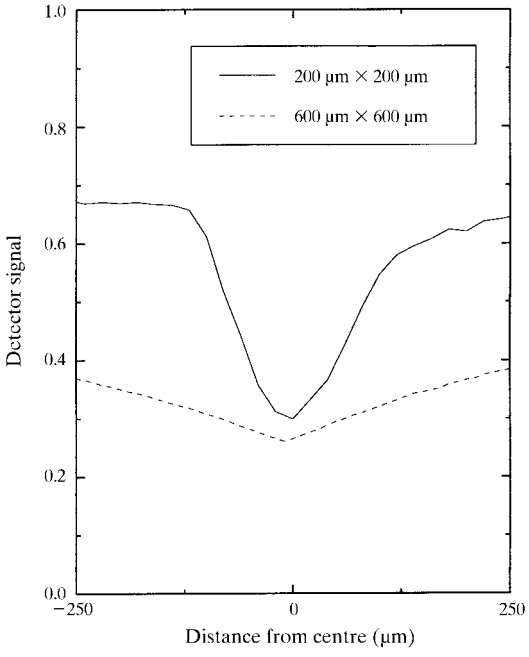

Figure 5
Evolution of the electrode currents in the centre of the BPM device, as a function of the beam size.

exhibits a very uniform response as the beam is scanned through the gold pads, and very sharp reductions in the signal are observed in the 500 μm gaps separating the electrodes. This region, where the current gradient is high with respect to position, enables accurate localization of the beam centre of gravity. Fig. 4 shows the currents plotted as a function of the beam position. Fig. 4(*a*) shows the evolution of the four currents when the beam scans the detector through the middle part of two gold pads. In this region the sensitivity to displacement approaches 11 pA μm^{-1}, and can easily be measured even without the use of synchronous detection. It can be noticed that no current is measured in one electrode when the beam does not touch it. Fig. 4(*b*) shows the same measurement performed on the central part of the detector. The fact that the baselines are not horizontal is due to a slight misorientation between the table displacement and the BPM axis, which had been aligned manually with the experimental set-up. Since the beam size used is much smaller than the electrode separation, this measurement has a very limited sensitivity. Despite this, the current variation reaches almost 0.1 pA μm^{-1} and can also be readily measured with the lock-in amplifier. Measurements with larger beam sizes have shown that the current values increase since the four quarters of the beam spot become closer to the gold pads, thus rendering position measurement easier. However, it is also clear that the larger the beam size, with respect to the electrode separation, the weaker the variation of the electrode currents with displacement (see Fig. 5). This results in a device for which the position resolution is beam-size dependent. The best resolution is obtained for beam-size values close to half of the inter-electrode separation, thus implying the use of different BPMs according to the beam size that is to be

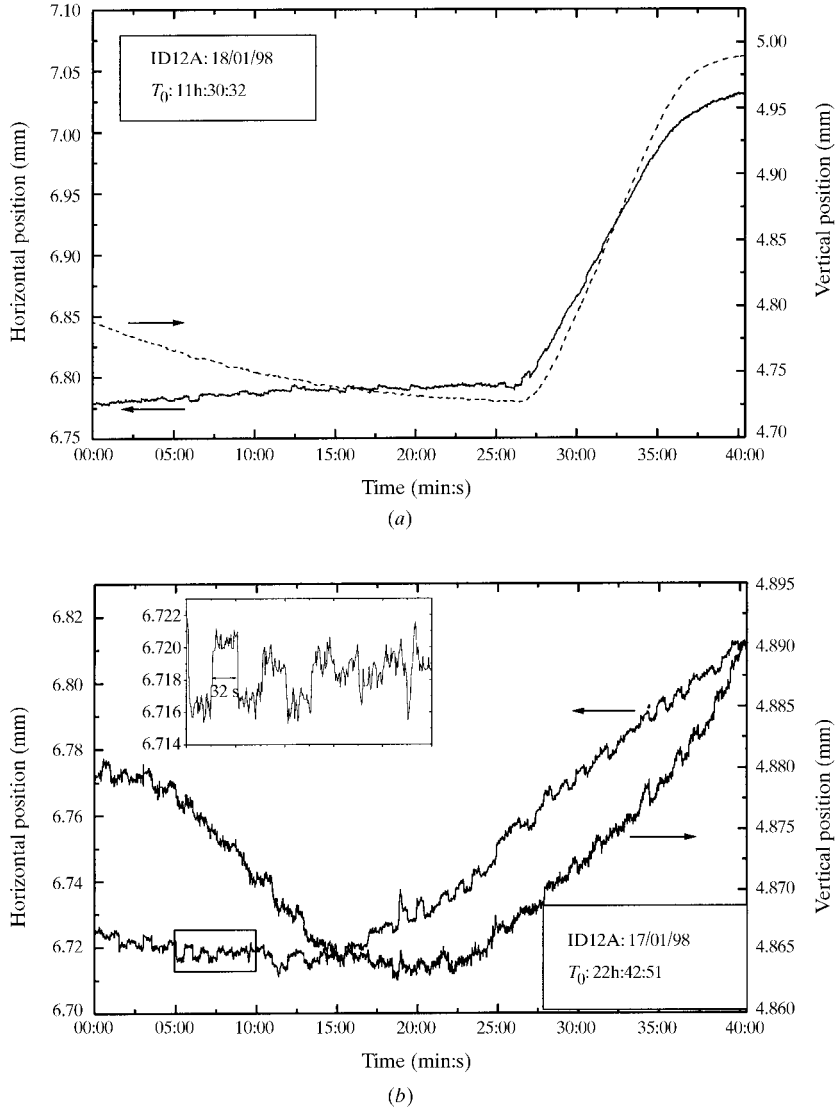

Figure 6
Time-scan measurements using the diamond BPM detector. Two records are obtained, revealing (*a*) unusual and (*b*) typical beam-position shifts. Beam energy is 4 keV, beam size is 200 μm × 200 μm. The use of a semi-transparent BPM allows the correction of those shifts.

monitored. This could be overcome using resistive readout devices, *i.e.* with a resistive layer (*e.g.* amorphous silicon or graphite) on the diamond surface, that results in current division among the four electrodes. Such a device would exhibit a response that is independent of the beam size, without dramatic resolution loss.

Furthermore, Fig. 4(*a*) points out that since the four currents are dropping substantially in the central region, the signal used for normalization, *i.e.* the sum of the four electrode signals, also drops consequently, and thus a significant increase of the signals can be observed on the two other plots that are not in the beam. This experimental artefact disappears when the electrode separation is reduced with respect to the beam size.

4.2. *Probing of the beam instabilities*

After calibration of the electrode currents with respect to the beam position, the diamond BPM was used to characterize the stability of the beamline position over relatively long time periods. Fig. 6 shows the evolution of the horizontal and vertical positions of the X-ray beam during 40 min scans. The curves provide clear evidence of beam instabilities. For example, Fig. 6(*a*) shows a sudden 200 μm beam shift that may cause beam losses to users or may render a measurement obsolete if it occurs during an experiment. However, such significant displacements are quite rare. Fig. 6(*b*) shows a smaller beam-position shift of the order of 40 μm over 20 min. Closer observation (see insert) reveals periodical shifts that correspond to the global feedback period of 32 s of the electron beam position in the storage ring. Displacements smaller than 2 μm can clearly be observed, and illustrate the excellent performance of the diamond BPM.

These beam instabilities can be extremely detrimental to experiments where the interaction position of the beam is crucial. For example, for XAFS experiments with a highly heterogeneous sample or for diffraction experiments on very small crystals, a displacement may result in severe errors. The direct measurement of the beam position with a semi-transparent diamond BPM would thus enable simultaneous correction of these effects during data acquisition.

5. Conclusions

A beam-position diamond detector has been fabricated and tested on ESRF beamlines. It demonstrates the unique feature of enabling position measurements with low attenuation of X-ray photons, thus allowing real-time monitoring of the beam with excellent position sensitivity. Real-time measurements of the beam position have given clear evidence of instabilities during the experiments. Knowledge of the beam-position instabilities may eventually allow its effects on the data to be corrected during the analysis, thus constituting a major breakthrough in the quality of experiments. Other applications are anticipated such as the control and feedback of the beamline optics. Further work is in progress where resistive layers are studied in order to replace the four-quadrant structure, thus enabling position measurements with a resolution that becomes independent with the beam size.

We thank S. Feite from the ID26 support team for technical help. This work was supported by the ESRF.

References

Bergonzo, P., Foulon, F., Marshall, R. D., Jany, C., Brambilla, A., McKeag, R. D. & Jackman, R. B. (1998). *IEEE Trans. Nucl. Sci.* **45**(3), 370–373.

Foulon, F., Bergonzo, P., Borel, C., Marshall, R. D., Jany, C., Besombes, L., Brambilla, A., Riedel, D., Museur, L., Castex, M. C. & Gicquel, A. (1998). *J. Appl. Phys.* **84**(9), 5531–5536.

Foulon, F., Bergonzo, P., Brambilla, A., Jany, C., Guizard, B. & Marshall, R. D. (1998). *MRS Proc.* **487**, 591–596.

Franklin, M., Fry, A., Gan, K. K., Han, S., Kagan, H., Kanda, S., Kania, D., Kass, R., Kim, S. K., Malchow, R., Morrow, F., Olsen, S., Palmer, W. F., Pan, L. S., Sannes, F., Schnetzer, S., Stone, R., Sugimoto, Y., Thomson, G. B., White, C. & Zhao, S. (1992). *Nucl. Instrum. Methods*, A**315**, 39–42.

Gauthier, C., Goujon, G., Feite, S., Moguiline, M., Braichovich, L., Brookes, N. B. & Goulon, J. (1995). *Physica B*, **208/209**, 232–234.

Gildenblat, G. H., Grot, S. A. & Badzian, A. (1991). *Proc. IEEE*, **79**(5), 647–665.

Jany, C., Bergonzo, P., Foulon, F., Tardieu, A. & Gicquel, A. (1998). *Proceedings of the 5th International Symposium on Diamond Materials*, edited by J. L. Davidson, W. D. Brown, A. Gicquel, B. V. Spitsyn & J. C. Angus. Pennington, NJ: Electrochemical Society.

Jany, C., Foulon, F., Bergonzo, P. & Marshall, R. D. (1998). *Diamond Relat. Mater.* **7**(7), 951–956.

Kania, D. R., Landstrass, M. I., Plano, M. A., Pan, L. S. & Han, S. (1993). *Diamond Relat. Mater.* **2**(5–7), 1012–1019.

Kania, D. R., Pan, L. S., Bell, P., Landen, O. L., Kornblum, H., Pianetta, P. & Perry, M. D. (1990). *J. Appl. Phys.* **65**, 124–130.

Manfredotti, C., Fizzotti, F., Vittone, E., Bistolfi, S., Boero, M. & Polesello, P. (1994). *Nucl. Instrum. Methods*, B**93**, 516–520.

Marinelli, M., Milani, E., Paoletti, A., Tucciarone, A., Rinati, G. V., Randazzo, N., Potenza, R., Pillon, M. & Angelone, M. (1998). *Diamond Relat. Mater.* **7**, 519–522.

Sakae, H., Aoyagi, H., Oura, M., Ohata, T., Shiwaku, H., Yamamoto, S., Sugiyama, H., Tanabe, K., Kobashi, K. & Kitamura, H. (1997). *J. Synchrotron Rad.* **4**, 204–209.